IOPscience iopscience.iop.org

Home Search Collections Journals About Contact us My IOPscience

Valence electron rules for prediction of half-metallic compensated-ferrimagnetic behaviour of Heusler compounds with complete spin polarization

This article has been downloaded from IOPscience. Please scroll down to see the full text article.

2006 J. Phys.: Condens. Matter 18 6171

(http://iopscience.iop.org/0953-8984/18/27/001)

View the table of contents for this issue, or go to the journal homepage for more

Download details:
IP Address: 129.252.86.83
The article was downloaded on 28/05/2010 at 12:13

Please note that terms and conditions apply.

INSTITUTE OF PHYSICS PUBLISHING JOURNAL OF PHYSICS: CONDENSED MATTER

J. Phys.: Condens. Matter **18** (2006) 6171–6181 doi:10.1088/0953-8984/18/27/001

Valence electron rules for prediction of half-metallic compensated-ferrimagnetic behaviour of Heusler compounds with complete spin polarization

Sabine Wurmehl, Hem C Kandpal, Gerhard H Fecher and Claudia Felser

Institut für Anorganische Chemie und Analytische Chemie, Johannes Gutenberg-Universität, 55099 Mainz, Germany

E-mail: felser@uni-mainz.de

Received 10 February 2006
Published 23 June 2006
Online at stacks.iop.org/JPhysCM/18/6171

Abstract

In this work, a rule for predicting half-metallic compensated-ferrimagnets in the class of Heusler compounds will be described. This concept results from combining the well-known Slater–Pauling rule with the Kübler rule. The Kübler rule states that Mn on the Y position in Heusler compounds tends to a highly localized magnetic moment. When strictly following this new rule, some candidates in the class of Heusler compounds are expected to be completely compensated-ferrimagnetic but with a spin polarization of 100% at the Fermi energy. This rule is applied to three examples within the class of Heusler compounds. All discussion of the materials is supported by electronic structure calculations.

A material with complete spin polarization at the Fermi energy (ϵ_F) is metallic with respect to one spin direction and semiconducting or insulating with respect to the other. This class of materials is called half-metallic ferromagnets [1]. The ternary compound NiMnSb was the first compound predicted to have this particular electronic structure [1]. The first half-metallic ferromagnets in the class of Heusler compounds were predicted by Kübler *et al* (Co_2MnAl, Co_2MnSn) [2]. Ishida *et al* later confirmed the occurrence of half-metallic ferromagnetism in Co_2-based Heusler compounds by first-principles calculations [3].

Heusler compounds are ternary X_2YZ compounds crystallizing in the $L2_1$ structure. The crystal lattice belongs to the spacegroup $Fm\bar{3}m$. X and Y are usually transition metals, while Z is a main group element. X (the more electronegative element) occupies the Wykhoff position $8c$ ($\frac{1}{4}\frac{1}{4}\frac{1}{4}$), Y is on $4b$ ($\frac{1}{2}\frac{1}{2}\frac{1}{2}$), and Z is on $4a$ (0 0 0). In the case of *XYZ* compounds with only half-filled X sites, the $C1_b$ structure is obtained that belongs to $F\bar{4}3m$.[1]

[1] These compounds are sometimes named half-Heusler compounds. This name is not used here to respect the different symmetry of the lattice.

 © 2006 IOP Publishing Ltd Printed in the UK

In 1991, de Groot [4] predicted the Heusler compound MnCrSb to exhibit ferrimagnetic coupling with compensating magnetic moments and 100% spin polarization at ϵ_F. This class of material was, unfortunately, called half-metallic antiferromagnets. Two cases of this rather unusual antiferromagnetism may occur in the cubic systems under investigation in [4] and here. In $C1_b$ compounds, the moments of two different atoms with the same site symmetry in the paramagnetic state (T_d) compensate, like the moments of Mn and Cr in MnCrSb. In DO_3 compounds, the moments of the same type of atoms with different site symmetry in the paramagnetic state (T_d and O_h) compensate, like in Mn_3Ga as reported below. Accordingly, in $L2_1$ compounds the kind of atom and local site symmetry are both different. However, all those materials principally do not fulfil the symmetry requirements needed to be an antiferromagnet. In normal antiferromagnets, the compensating magnetic moments originate from the same kind of atom. A distinct symmetry element (combined with time inversion operation) relates the magnetic moments on the different sites with oppositely oriented moments. Such a symmetry is absent for the materials discussed in this work. In the materials under investigation, the magnetic moments on crystallographically different lattice sites compensate at a particular band filling (note the absence of a symmetry element linking these sets of atomic positions to one another—even in the paramagnetic state). This is the configuration encountered for ferrimagnetic materials at the compensation point and is entirely different from an antiferromagnet. The only common property between this type of ferrimagnets and the regular antiferromagnets is the vanishing overall magnetic moment in the ground state and some related physical properties.

In regular compensated ferrimagnets, the compensation is not a ground-state property but a thermally excited state. Therefore, the class of ferrimagnetic materials with complete spin polarization at ϵ_F and a ground state with compensated magnetic moments will be called half-metallic completely compensated-ferrimagnets (HMCCFs) in the following.

Unfortunately, the suggested material MnCrSb does not crystallize in the required $C1_b$ structure [5]. As presented by van Leuken and de Groot [6], another possible material is $Fe_8MnV_7Sb_7In$, a Heusler-type quintinary compound. Quintinary compounds are difficult to synthesize in their stoichiometric form. This means that MnCrSb as well as $Fe_8MnV_7Sb_7In$ are mainly interesting from a theoretical point of view [7]. Other half-metallic materials with compensated moments have been expected in the class of double perovskites [7–9] as well as the class of thiospinels [10]. However, experiments have shown that, due to disorder, the predicted material $LaAVMoO_6$ (A = Ca, Sr, Ba) is a normal metallic ferrimagnet [11].

HMCCFs are supposed to have a potential advantage over half-metallic ferromagnets for some technical applications, because they have no stray field and are much less affected by external magnetic fields. They could be used as sensors in spin polarized scanning tunnelling microscopes for measuring the spin polarization of samples without perturbing the domain structures [4]. In particular, half-metallic materials with full spin polarization and without stray magnetic fields may be useful for advanced 'spin electronic' devices [4, 6]. The HMCCFs were also predicted as a base for a new type of superconductor that has only one superconducting spin channel, the so-called single-spin superconductor [12].

Many of the Heusler compounds fulfil the Slater–Pauling rule [13, 14], which states that the magnetic moment is determined by the mean number of valence electrons per atom [2, 13–15]. This rule can be specified for ordered compounds [2, 15] such that the magnetic moment (m, in μ_B) can be calculated by subtracting 18 for the $C1_b$ or 24 for the Heusler compounds from the accumulated number of valence electrons (N_V) in the unit cell. It follows immediately that $C1_b$ compounds with 18 valence electrons and Heusler compounds with 24 valence electrons are not ferromagnetic. The prototypes for non-ferromagnetic compounds are CoTiSb [16] ($N_V = 18$) and Fe_2VAl [17] ($N_V = 24$). Both compounds are semiconductors [16, 17].

Another prototype for a non-ferromagnetic Heusler compound with 24 valence electrons may be considered. Mn_2VAl is a half-metallic ferromagnet with 22 valence electrons [18]. In this compound, Mn occupies the X position. Substituting half of the Mn by Co (on the X position!) also results in a non-ferromagnetic compound ($(Mn_{0.5}Co_{0.5})_2VAl$) with 24 electrons [19]. This implies that mixed Heusler compounds with 24 valence electrons also follow the Slater–Pauling rule.

Besides the Slater–Pauling rule, another rule, as described by Kübler *et al* [2], states that the properties of Mn on the Y position in the Heusler compounds must be included. This rule states that Mn on the Y position in Heusler compounds tends to have a high, localized magnetic moment [2, 18, 20]. According to electronic structure calculations, in the $C1_b$ compounds, Mn on the Y position has a magnetic moment of approximately 4 μ_B. Mn may be formally described as Mn^{3+}, with a d^4 configuration. In accordance with the itinerant character of the 3d transition metals, one will find a lower magnetic moment, even if there is a partial localization of the d electrons.

As an example, the Slater–Pauling rule can be applied to NiMnSb [1], which has 22 valence electrons and a total magnetic moment of 4.0 μ_B. Suga *et al* [21] reported a local magnetic moment of 3.62 μ_B at the Mn site, while Ni and Sb have small magnetic moments. Large magnetic moments of Mn on the Y position in the Heusler compounds X_2YZ have also been found [2, 18, 20]. A detailed list of magnetic moments located at the Mn Y site in Heusler compounds is given in [2]. As already mentioned above, the Heusler compound $(Mn_{0.5}Co_{0.5})_2VAl$, with 24 valence electrons and Mn on the X position, is not ferromagnetic, indicating the importance of the role of the atom on the Y position for half-metallic completely compensated-ferrimagnetic character.

A combination of the Slater–Pauling rule [13, 14] and the Kübler rule [2], given above, leads to a rule for the prediction of half-metallic completely compensated-ferrimagnetism in Heusler compounds with 24 valence electrons and with Mn on the Y position. In these compounds, the two atoms on the X site have to compensate the magnetic moment of the Mn at the Y site. This rule is in agreement with the approach of de Groot in [4]. In [4], the above-mentioned rule was implicitly applied in the case of MnCrSb, resulting in the prediction of the completely compensated magnetic moments in MnCrSb. For convenience, the Mn on the Y position (4b) with the cubic environment will be referred to as MnI and the atom on the X position (8c) with tetrahedral environment will be indicated by the numeral II.

Potential half-metallic completely compensated-ferrimagnets were considered. Mn has to be the more electropositive transition metal in order to occupy the Y position. Possible transition metals to occupy the X position are the more electronegative elements Fe, Co, Ni, Cu, and Zn, as well as Mn itself. All those transition metals have seven (Mn) or more valence electrons. The accumulated number of electrons is limited to 24 to result in a zero net moment. This condition allows only a few possible models, namely the binary Mn_2MnZ compounds, with Z being a IIIa element. Thus, the binary (Heusler[2]) compounds Mn_3Z are the simplest possible models (Z = Al or Tl are not yet reported; Z = In [22, 23] and Z = Ga [24–26]). They may be the most practical candidates for checking the HMCCF state, because they consist of only two different kinds of atoms.

To check the validity of the rules found semi-empirically, self-consistent field calculations were performed using the full potential linear augmented plane wave (FLAPW) method, as provided by WIEN2K [27]. The exchange–correlation functional was evaluated within the generalized gradient approximation (GGA), using the Perdew–Burke–Ernzerhof [28]

[2] The ternary X_3Z compounds resulting from Y = X are known as DO_3 compounds. They are usually not included in the class of Heusler compounds.

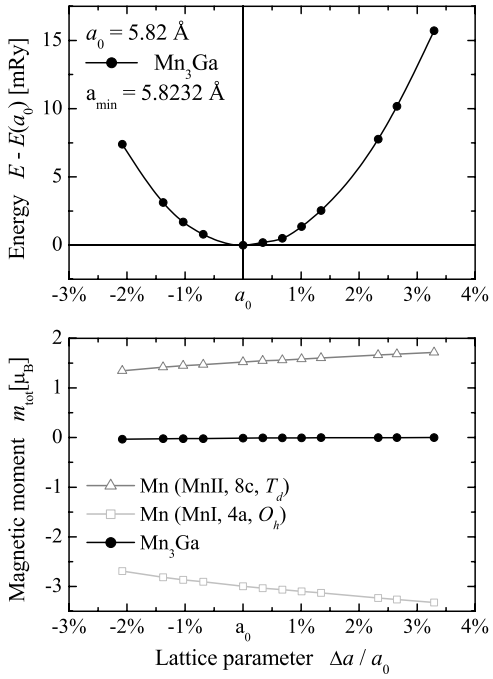

Figure 1. Structural optimization for Mn_3Ga. The optimized lattice constant (upper panel) and the magnetic moment (lower panel) are shown as functions of the of the lattice parameter.

parametrization. The energy threshold between the core and the valence states was set to −81.6 eV. The muffin-tin radii (R_{MT}) were taken in the range of 2.3–2.36 a_{Bohr} (a_{Bohr} = 0.529 177 Å), this resulted in nearly touching spheres. $R_{MT} \times k_{max} = 7$ was used for the number of plane waves. The expansion was taken up to $l = 10$ inside the muffin-tin spheres. The self-consistent calculations employed a grid of 455 k points from a 25 × 25 × 25 mesh in the irreducible part of the Brillouin zone. A 22 × 22 × 15 mesh was used for integration of the tetragonal cells, leading to 528 irreducible k points. A similiar mesh leads to 968 irreducible k points for the orthorhombic cell. The energy convergence criterion was set to 10^{-5}, and simultaneously the charge convergence was set to 10^{-3}. It should be noted that care has to be taken while initializing the calculations. Slight differences in the initial parameters cause the calculations to converge to an inappropriate minimum of the total energy. This may result in wrong conclusions about the ground state.

For comparison, the linear muffin tin orbital (LMTO) method [29] and the Korringha–Kohn–Rostocker (KKR) method [30] were used. In most cases, it was found that the results did not depend on a particular method for the electronic structure calculations, however the methods with spherical potentials seem to underestimate the gap in the minority states. In some cases, only a pseudo-gap was found when using spherical potentials.

Mn_3Ga is the only one of the four binary compounds given above that is reported to order in the same space group ($Fm\bar{3}m$) as Heusler compounds [24–26]. First of all, a structural optimization was performed for Mn_3Ga by minimizing the total energy as a function of the volume. The optimized lattice parameter is $a = 5.8232$ Å (see figure 1). For this lattice parameter, the calculation reveals nearly complete compensation of the magnetic moments and an HMCCF character. A change in the lattice parameter by up to ±3% only changes the local

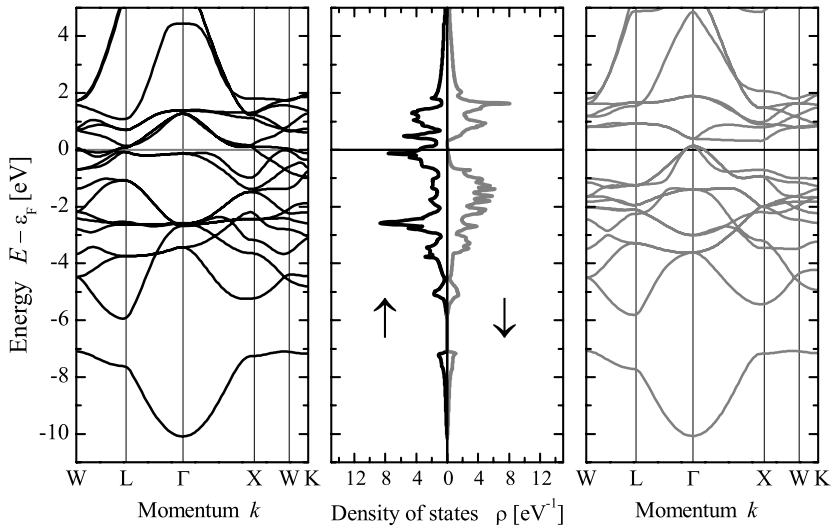

Figure 2. Band structure (right and left panels) and DOS (middle panel) of Mn_3Ga. The band structure, as well as the DOS, clearly exhibits 100% spin polarization at ϵ_F.

magnetic moments on the two different Mn sites. As shown in the lower panel of figure 1, an overall increase in the lattice parameter slightly increases the magnetic moment of the MnII position and decreases the magnetic moment of the MnI position. The total magnetic moment of zero, as a sum of the site-specific Mn moments, remains unaffected. This result is expected, because the magnetic moment is very stable in the range of the gap and similar behaviour is observed during the lattice parameter optimization of the Heusler compound Co_2FeSi [31–33].

The optimized lattice parameter was used to calculate the details of the electronic structure of Mn_3Ga (figure 2). The obtained minority density of states (DOS) clearly shows a gap at the Fermi energy (ϵ_F), while the majority DOS exhibits states at ϵ_F.[3] As shown by Pickett in [12], the DOS follows the idealized DOS for a half-metallic state. The majority DOS shows a very narrow peak at -2.6 eV. These highly localized electrons also show up in the majority channel of the band structure as very flat bands through all high-symmetry points in the Brillouin zone. In addition, the band structure indicates that the gap in the minority channel is a real gap and not a pseudo-gap.

Figure 3 shows the integrated DOS (number of states, NOS) of Mn_3Ga. Both spin channels contain 12 electrons. Up to -4.5 eV, the NOS is symmetric for both spin channels. This is the range of the low-lying sp bands. At higher energies, the DOS for both spin channels starts to differ. The most interesting difference occurs near ϵ_F. As a result of the gap, the minority channel exhibits a plateau at approximately 0.75 eV around ϵ_F. In the range of this plateau, the number of electrons is constant.

The calculated magnetic moments of Mn_3Ga are $m_I = 3.03\ \mu_B$ for Mn on the Y position (MnI) and $m_{II} = -1.54\ \mu_B$ for each Mn on the X position (MnII). The remaining part is found at the Ga atoms and in the interstitial.

Figure 4 shows the partial DOS of Mn_3Ga. The Mn on the X position mainly dominates the minority channel below ϵ_F and the majority channel near and, in particular, above ϵ_F. For MnI, there are no states at ϵ_F in the majority channel. The main contributions of the MnI lie in the

[3] In Mn_3Ga, there are 12 electrons in both spin channels, so it is not possible to define the majority and minority spin channels by the number of electrons.

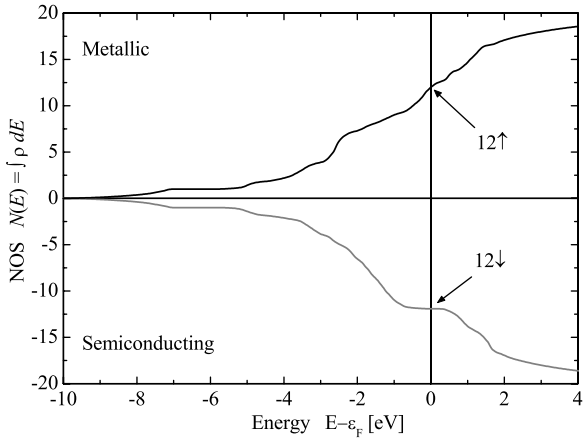

Figure 3. Integrated DOS of Mn_3Ga (NOS). The minority channel exhibits a plateau at ϵ_F.

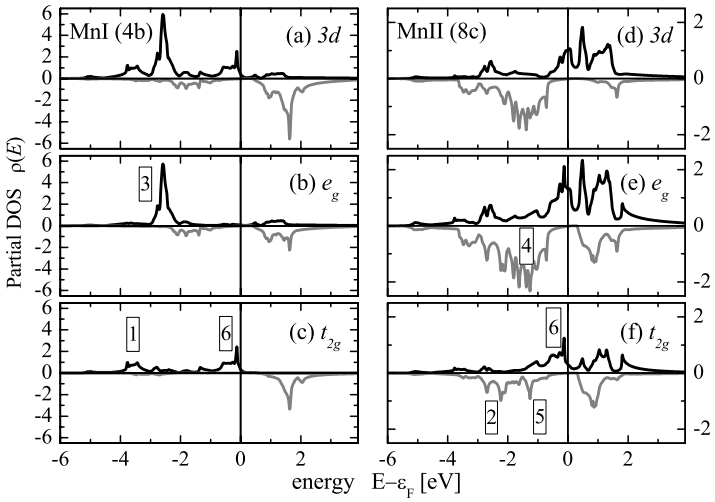

Figure 4. Partial DOS of Mn_3Ga. The DOS of Mn on the X position (MnII) (panels (d)–(f)) and the DOS of Mn on the Y position (MnI) (panels (a)–(c)) are shown. Panels (a) and (d) show the Mn 3d DOS. The Mn d orbitals are split in e_g (panels (b) and (e)) and in t_{2g} (panels (c) and (f)). The low-lying sp bands mainly belong to the Ga atoms (not shown here). The numbers indicate the corresponding states shown in figure 5.

majority channel below ϵ_F and in the minority channel above ϵ_F. As expected, MnI contributes to the parts of the DOS that are exactly the opposite of the parts to which Mn atoms on the X position contribute. In particular, the DOS of MnII is rather widely spread, while the DOS of MnI has a narrow peak in the e_g orbitals at -2.6 eV. This narrow peak results in a localized magnetic moment. The MnI as well as the MnII show narrow peaks approximately -0.2 eV below ϵ_F in the t_{2g} states in the majority channel. These states form the MnI–MnII bond, which corresponds to the flat band in the Γ–L direction at -0.2 eV below ϵ_F.

Figure 5 shows the distribution of the magnetic moment as a function of energy. The black line represents the total distribution of the magnetic moment of Mn_3Ga. The light-grey line shows the distribution of the magnetic moments of the MnI site and the dark-

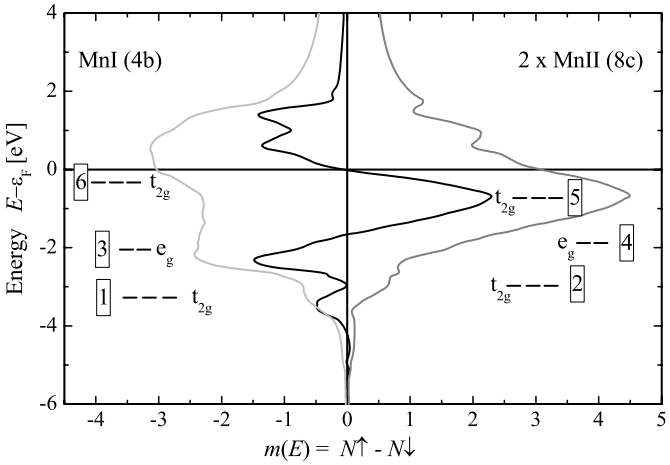

Figure 5. Magnetic moment as a function of energy, with indicated orbitals. The light-grey curve represents the magnetic contribution of MnI and the dark-grey curve shows the MnII contribution. The black line corresponds to the magnetic distribution, which originates from the total DOS. The numbers indicate the corresponding states as given in figure 4.

grey line represents the distribution of the magnetic moments of the MnII site. Because of compensating magnetic moments, the magnetic moment is zero at the nodes of the magnetic moment distribution curve. Each of these orbitals carries a number that indicates the band that contributes to the partial DOS (see also figure 4). The first contributing orbitals are the t_{2g} majority orbitals of the MnI t_{2g} at approximately -3.8 eV. The maximum of this peak is at -3.5 eV. At this energy, MnII starts to compensate this magnetic moment with the t_{2g} minority orbitals. These magnetic moments exactly compensate each other at -2.97 eV at ϵ_F. The next magnetic contribution arises from the MnI e_g majority orbitals. The electrons in this orbital are highly localized and the magnetic moment in this orbital is approximately 2 μ_B. At -2.4 eV, the e_g minority orbitals of MnII start to contribute, cancelling the magnetic moment of the MnI e_g orbitals at -1.67 eV. The magnetic moment at MnII arises from t_{2g} minority electrons and is exactly compensated at ϵ_F by t_{2g} majority electrons located at MnI, leading to a magnetic moment of zero at ϵ_F. The magnetic moment of the MnI at the Y position adds up to about 3 μ_B, while each of the two MnII at the X position have a magnetic moment of -1.5 μ_B. As mentioned above, the highly localized electrons at -2.6 eV in the MnI e_g orbital have a local magnetic moment of 2 μ_B. The remaining 1 μ_B of MnI is delocalized in the MnI t_{2g} orbitals, and the magnetic moment on the MnII site is considerably delocalized.

In the next section, the rule for the prediction of half-metallic completely compensated-ferrimagnetism is applied to ternary and quaternary compounds. These have the advantage of being constructed from already-known existing Heusler compounds. In addition, the chances for an experimental realization of a practicable HMCCF material are improved if the end members of the doped compounds exist as in the cases given below.

The $Mn_{3-x}V_xSi$ system was found to be a potential candidate for half-metallic ferrimagnetism with completely compensated magnetic moments. Mn_3Si has 25 valence electrons which, according to the Slater–Pauling rule, results in an expected magnetic moment of about 1 μ_B. Mn_3Si is reported to be an antiferromagnet [34–36]. Mn_2VSi has 23 valence electrons and therefore it also has a predicted magnetic moment of 1 μ_B, but with a gap in the majority DOS. For further details regarding the calculated local moments, see table 1.

Table 1. Magnetic moments in proposed HMCCFM compounds. Total spin magnetic moments, m_{tot}, are given per unit cell. m_X and m_Y are the element-specific magnetic moments on X and Y sites, respectively. All magnetic moments are given in μ_B. Note that a small part of the magnetic moment may also be localized outside the muffin-tin spheres and thus cannot be attributed to one of the atoms.

Compound	N_V	m_{tot}	m_X	m_Y
Mn_3Al	24	0.00	−1.42	2.84
Mn_3Ga	24	−0.01	−1.54	3.03
Mn_2VSi	23	0.97	−0.70	0.39
Mn_3Si	25	1.00	−0.88	2.69
$Mn_2(Mn_{0.5}V_{0.5})Si$	24	0.00	MnII: −0.88	MnI: 2.84; V: 0.52
Mn_2VAl	22	2.00	−1.52	0.95
Fe_2MnAl	26	2.00	−0.31	2.62
$(MnFe)(Mn_{0.5}V_{0.5})Al$	24	0.00	MnII: −1.53; Fe: −0.18	MnI: 2.79; V: 0.56

Table 2. Minority band gaps. E_{VBmax} and E_{CBmin} are the extremal energies of the lower and upper bands defining the position of the gap with respect to the Fermi energy. ΔE is the size of the gap in the minority states. a is the lattice parameter used for the calculations. For the mixed compounds, the corresponding lattice parameter a_c is given.

Compound	a (Å)	E_{VBmax} (eV)	E_{CBmin} (eV)	ΔE (meV)
Mn_3Al	5.804	−0.12	0.42	540
Mn_3Ga	5.823	0.14	0.32	180
$Mn_2(Mn_{0.5}V_{0.5})Si$	5.82	−0.01	0.22	230
$(MnFe)(Mn_{0.5}V_{0.5})Al$	5.829	−0.06	0.32	380

A mixture of 50% Mn_3Si (25 valence electrons) and 50% Mn_2VSi (23 valence electrons) results in $Mn_2(Mn_{0.5}V_{0.5})Si$. The X site is completely occupied by MnII, while MnI and V share the Y site. The accumulated number of valence electrons is 24. This compound is also used as a test case whether a partial occupation of the Y position by Mn leads already to a localized magnetic moment and to a HMCCF state.

A supercell with an overall stoichiometry given by Mn_4MnVSi_2 in a tetragonal primitive cell was used to model the structure of $Mn_2(Mn_{0.5}V_{0.5})Si$. The spacegroup is $P/4mmm$ with a lattice parameter ratio of $c/a = \sqrt{2}$. The lattice parameters are $a = 4.115$ Å and $c = a_c = 5.82$ Å, where a_c is the lattice parameter of the initially cubic $L2_1$ cell. The Mn related to the X position occupies the $(\frac{1}{2}\ 0\ \frac{1}{4})$ position in the supercell, the Mn dedicated to the Y position is now on $(\frac{1}{2}\frac{1}{2}\frac{1}{2})$, and V is placed on (0 0 0). In this supercell, the Si atoms occupy two different positions, being located at $(\frac{1}{2}\ \frac{1}{2}\ 0)$ and $(0\ 0\ \frac{1}{2})$.

The result of the electronic structure calculation is an HMCCF (see also tables 1 and 2). Figure 6 shows the band structure and the DOS of $Mn_2(MnV)_{0.5}Si$, which fits the DOS for an HMCCF, as shown in [12]. The local magnetic moments compensate each other so that the total magnetic moment of $Mn_2(Mn_{0.5}V_{0.5})Si$ vanishes. The constituent magnetic moments for the referred compounds are listed in table 1. Apparently, a partial occupation of the Y position by Mn is sufficient to enforce a localized magnetic moment and results in an HMCCF. The minority bands exhibit a clear gap in the vicinity of the Fermi energy. The density of states and band structure of the supercell are, however, too complicated to be analysed in detail as for the example of Mn_3Ga given above.

In the next step, the quaternary system $Mn_{2-x}Fe_xMn_{1-x}V_xAl$ was analysed to verify the new rule. Mn_2VAl is a half-metallic ferromagnet with 22 valence electrons [18]. Assisted by

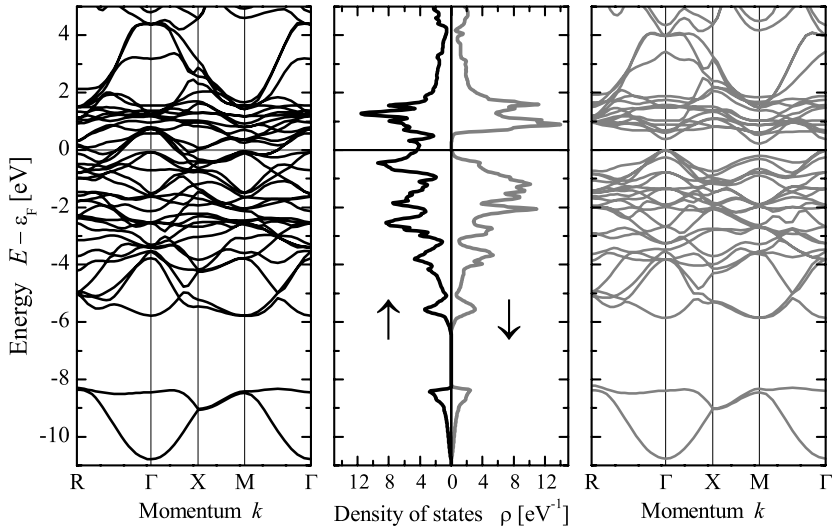

Figure 6. Spin-resolved density of states and band structure of $Mn_2(Mn_{0.5}V_{0.5})Si$. The calculations were performed for a tetragonal cell.

calculations, the rule gives a magnetic moment of 2 μ_B for Mn_2VAl. This result is in agreement with the result obtained by Weht and Pickett [18]. Measurements in [1] and [37] confirm this value. In agreement with the Slater–Pauling rule, Fe_2MnAl is also a half-metallic ferromagnet with 26 valence electrons and a calculated magnetic moment of 2 μ_B. A 1:1 mixture of both compounds again results in a compound with 24 valence electrons, an expected total magnetic moment of zero, and with anti-parallell coupled local magnetic moments (see tables 1 and 2).

The $(MnFe)(Mn_{0.5}V_{0.5})Al$ structure was modelled using an orthorombic supercell ($Pmmm$) with $a = b = c/\sqrt{2}$ using $c = a_c = 5.829$ Å and an overall stoichiometry of $Mn_3Fe_2VAl_2$. As can be seen from the calculated electronic structure (shown in figure 7), $(MnFe)(Mn_{0.5}V_{0.5})Al$ is 100% spin polarized at ϵ_F. The calculated magnetic moments (see table 1) reveal an anti-parallel coupling of the moments on Y and X positions. Again, a partial occupation of Mn is sufficient to enforce a localized magnetic moment on the Y position, leading to half-metallic completely compensated-ferrimagnetism.

Table 2 summarizes the properties of the minority gaps of the investigated materials. Given are the extremal energies of the bands, involving the gap and its resulting size. Mn_3Al shows a relatively large minority gap of 540 meV. The gap is reduced in the iso-valent compound Mn_3Ga to 180 meV and vanishes for Mn_3In. Such a reduction of the gap in compounds with row 5 or 6 main group elements is very often observed in Heusler compounds.

In pure LSDA calculations at the optimized lattice parameter, the top of the Mn_3Ga minority valence band is slightly above ϵ_F (see also figure 2). This is probably due to the van Hove singularity at ϵ_F in the majority states which may lead to numerical problems while integrating the total charge. An increase in the volume by 5% reduces the size of the gap to $\Delta E = 30$ meV, and it vanishes completely for larger lattice parameters. The lattice parameter of the Heusler compounds is usually determined by the main group element. This is finally the cause why the gap vanishes in Mn_3In with a larger lattice parameter. The gap of Mn_3Al is considerably larger due to the smaller lattice parameter. It clearly involves the Fermi energy, as is also observed for the mixed compounds.

As already mentioned above, half-metallic materials with completely compensated moments are also found among double perovskites as well as thiospinels. Similar rules for

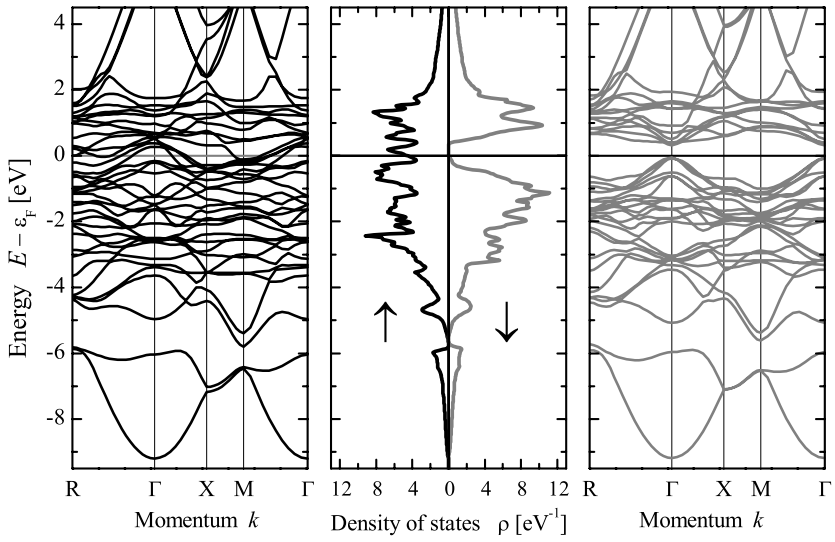

Figure 7. Electronic structure of (MnFe)($Mn_{0.5}V_{0.5}$)Al. The calculations were performed for an orthorhombic cell.

predicting HMCCF compounds may also exist within these classes of materials. For the double perovskites, a sequence of numbers (12, 14, 16) appears that leads to a total magnetic moment of zero. In addition, these materials contain two strongly localized magnetic moments with fixed valences. This apparently results in different conditions for the occurrence of half-metallic compensated-ferrimagnetism in double perovskites. The number of valence electrons required to form a non-magnetic ground state is 10 for the thiospinels.

In summary, a rule for predicting half-metallic completely compensated-ferrimagnetic behaviour is presented. This new rule is a combination of two well-known rules. The first of these, which is the Slater–Pauling rule, determines the total magnetic moment from the mean number of valence electrons. According to this rule, the half-metallic system of interest must have 24 valence electrons. The Kübler rule, which is the second of these rules, states that Mn in Heusler compounds always carries a high local magnetic moment at the Y site. A combination of these rules results in an easy concept for finding new compounds with half-metallic-type behaviour and completely compensated moments. Furthermore, it was found that even partial occupation of the Y position by Mn is sufficient to enforce a local magnetic moment on this site. The next step will be the synthesis and characterization of the above-mentioned compounds. The verification of their HMCCF-type character by the performance of appropriate experiments will follow later.

Acknowledgments

Financial support from the Deutsche Forschungsgemeinschaft (DFG, research group: FG 559; TP1, TP7) is gratefully acknowledged.

References

[1] de Groot R A, Müller F M, van Engen P G and Buschow K H J 1983 *Phys. Rev. Lett.* **50** 2024
[2] Kübler J, Williams A R and Sommers C B 1983 *Phys. Rev.* B **28** 1745

[3] Ishida S, Fujii S, Kashiwagi S and Asano S 1995 *J. Phys. Soc. Japan* **64** 2152–7
[4] de Groot R A 1991 *Physica* B **172** 45
[5] Wjngaard J H, Haas C and de Groot R A 1992 *Phys. Rev.* **45** 5395
[6] van Leuken H and de Groot R A 1995 *Phys. Rev. Lett.* **74** 7
[7] Pickett W E 1998 *Phys. Rev.* B **57** 10613
[8] Park J H, Kwon S K and Min B I 2002 *Phys. Rev.* B **65** 174401
[9] Min B I, Park J H and Park M S 2004 *J. Phys.: Condens. Matter* **16** S5509
[10] Park J H, Kwon S K and Min B I 2001 *Phys. Rev.* B **64** 100403
[11] Park J H and Min B I 2005 *Phys. Rev.* B **71** 052405
[12] Pickett W E 1996 *Phys. Rev. Lett.* **77** 3185
[13] Slater J C 1936 *Phys. Rev.* **49** 931
[14] Pauling L 1938 *Phys. Rev.* **54** 899
[15] Galanakis I, Dederichs P H and Papanikolaou N 2002 *Phys. Rev.* B **66** 174429
[16] Kouacou M A, Pierre J and Skolozdra R V 1995 *J. Phys.: Condens. Matter* **7** 7373
[17] Kato M, Nishino Y, Mizutani U and Asano S 2000 *J. Phys.: Condens. Matter* **12** 1796
[18] Weht R and Pickett W E 1999 *Phys. Rev.* **60** 13006
[19] Galanakis I and Dederichs P H 2005 Half-metallicity and Slater–Pauling behaviour *Halfmetallic Alloys* (*Lecture Notes in Physics* vol 676) ed I Galanakis and P Dederichs (Berlin: Springer)
[20] Buschow K H J and van Engen P G 1981 *J. Magn. Magn. Mater.* **25** 90
[21] Suga S and Imada S 1998 *J. Electron Spectrosc. Relat. Phenom.* **92** 1–9
[22] Browne J D, Hance N J, Johnston G B and Sampson C F 1978 *Phys. Status Solidi* a **49** K177
[23] Okamoto H 1990 *Bullet. Alloy Phase Diagram* **11** 303
[24] Meißner H-G and Schubert K 1965 *Z. Naturk.* **56** 523
[25] Bushow K H J, van Engen P G and Jongebreur R 1983 Magneto-optical properties of metallic ferromagnetic materials *J. Magn. Magn. Mater.* **38** 1–22
[26] Niida H, Hori T, Onodera H, Yamaguchi Y and Nakagawa Y 1996 *J. Appl. Phys.* **79** 5946
[27] Blaha P, Schwarz K, Madsen G K H, Kvasnicka D and Luitz J 2001 *WIEN2k, An Augmented Plane Wave + Local Orbitals Program for Calculating Crystal Properties* Karlheinz Schwarz, Techn. Universitaet Wien, Wien, Austria
[28] Perdew J P, Burke K and Ernzerhof M 1996 *Phys. Rev. Lett.* **77** 3865
[29] Jepsen O and Andersen O K 1998 *The Stuttgart Tight-Binding Lmto-Asa Program Version 4.7. (Stuttgart, 1998)*
[30] Ebert H 1999 Fully relativistic band structure calculations for magnetic solids formalism and application *Electronic Structure and Physical Properties of Solids. The Use of the LMTO Method* (*Lecture Notes in Physics* vol 535) ed H Dreysee (Berlin: Springer) pp 191–246
[31] Wurmehl S, Fecher G H, Kandpal H C, Ksenofontov V, Felser C, Lin H-J and Morais J 2005 *Phys. Rev.* B **72** 184434
[32] Wurmehl S, Fecher G H, Kandpal H C, Ksenofontov V, Felser C and Lin H-J 2006 *Appl. Phys. Lett.* **88** 1
[33] Kandpal H C, Fecher G H, Felser C and Schönhense G 2006 *Phys. Rev.* B **73** 094422
[34] Pfleiderer C, Boeuf J and von Lohneysen H 2002 *Phys. Rev.* B **65** 172404
[35] Pfleiderer C 2003 *Physica* B **329** 1085–6
[36] Boeuf J, Faisst A and Pfleiderer C 2003 *Acta Phys. Pol.* B **34** 395
[37] Rudd R E and Pickett W E 1998 *Phys. Rev.* B **57** 557